In-flight calibration of the Swift XRT effective area

G. Cusumano[*], S. Campana[†], P. Romano[†], V. Mangano[*], A. Moretti[†], A.F. Abbey[**], L.Angelini[‡], A.P. Beardmore[**], D.N. Burrows[§], M. Capalbi[¶], G. Chincarini[†,‖], O. Citterio[†], P. Giommi[††], M.R. Goad[**], O. Godet[**], G.D. Hartner[‡‡], J.E. Hill[‡], J.A. Kennea[§], V. La Parola[*], T. Mineo[*], D. Morris[**], J.A. Nousek[§], J.P. Osborne[**], K. Page[**], C. Pagani[†,§§], M. Perri[¶], G. Tagliaferri[†], F. Tamburelli[¶] and A. Wells[**]

[*]*INAF-Istituto di Astrofisica Spaziale e Fisica Cosmica di Palermo, Via Ugo La Malfa 153, 90146 Palermo, Italy*
[†]*INAF – Osservatorio Astronomico di Brera, Via Bianchi 46, 23807 Merate Italy*
[**]*Department of Physics and Astronomy, University of Leicester, University Road, Leicester LE1 7RH, UK*
[‡]*NASA-GSFC, Greenbelt, MD 20771, USA*
[§]*Department of Astronomy & Astrophysics, Pennsylvania State University, PA 16802, USA*
[¶]*IASI Science Data Center, via Galileo Galilei, 00044 Frascati, Italy*
[‖]*Università degli studi di Milano-Bicocca, Dip. di Fisica, Piazza delle Scienze 3, I-20126 Milano, Italy*
[††] *ASI Science Data Center, via Galileo Galilei, 00044 Frascati, Italy*
[‡‡] *Max-Planck-Institut für extraterrestrische Physik, Germany*
[§§]*Pennsylvania State University, 525 Davey Lab, University Park, PA 16802, USA*

Abstract. The Swift X-ray Telescope (XRT) is designed to make astrometric, spectroscopic and photometric observations of the X-ray emission from Gamma-Ray Bursts and their afterglows in the 0.2-10 keV energy band. Here we report some results on the in-flight calibration of the Swift XRT effective area obtained analysing observations of cosmic sources with different intrinsic spectra and using the on-ground calibration and ray-tracing simulations as a starting point. Our analysis includes the study of the effective area for different XRT operating modes.

Keywords: <Enter Keywords here>
PACS: <Replace this text with PACS numbers; choose from this list: `http://www.aip..org/pacs/index.html`>

INTRODUCTION

The Swift gamma-ray burst Explorer [**?**] includes in its payload a wide-field instrument, the gamma-ray (15-350 keV) Burst Alert Telescope (BAT, [**?**]) which detects the bursts, calculates their position to ~ 1–$4'$ accuracy and triggers an autonomous slew of the observatory, and two narrow-field instruments, the X-Ray Telescope (XRT, [**?**]), which operates in the 0.2–10 keV energy range and can provide $\sim 3''$ positions, and the Ultraviolet/Optical Telescope (UVOT, [**?**]), which operates in the 1700–6000Å wavelength range and provides $\sim 0.5''$ positions.

The XRT is a focusing X-ray telescope that utilizes the third flight mirror module (FM3) developed for the JET–X program [**?**] and consists of 12 nested, cofocal and coaxial mirror shells arranged in a Wolter I configuration. The mirror diameters range

from 191 mm to 300 mm and the focal length is 3.5 m, with a total field of view of $\sim$ 40 arcminutes (50% vignetting level, 1.5 keV). The XRT detector was designed for the EPIC MOS instruments on XMM–Newton and is a MAT-22 CCD consisting of 600 x 602 pixels (40μm $\times 40\mu$m) and being the plate scale of $2.36''$/pixel, it covers an effective field of view of $\sim 24'$ [**?**]. The XRT Point Spread Function, as measured during the on-ground calibration, is $18''$ and $22''$ (HEW) at 1.5 keV and 8.1 keV, respectively. The XRT effective area is $\sim$135 cm^2 at 1.5 keV and $\sim$ 65 cm^2 at 8.1 keV, and depends on XRT read-out modes and grade selection. Four calibration sources are located at the corners of the detector to monitor the spectral resolution as the mission progresses.

XRT supports four different read-out modes to cover the dynamic range and rapid variability expected from GRB afterglows. The switch between modes is performed automatically in order to minimize pile-up and optimize the collected information as the flux of the afterglow diminishes. In Imaging mode the XRT produces an integrated image (no X-ray event recognition takes place) which, for a typical GRB flux, is highly piled up. No spectroscopy is therefore possible, but a very accurate position and a good flux estimate can be obtained. The Photodiode mode (PD) is designed for very bright sources and for high timing resolution. Depending on the source count rate, two telemetry formats are available; at high fluxes (<60 Crab) data are telemetred in Piled-up PD (PuPD) mode in which data are piled-up and spectral information is degraded; at lower fluxes (< 3 Crab) data are telemetred in Low Rate PD (LrPD) and full spectral information is available. The spectra of the four corner sources are superimposed on the spectra of the astronomical sources. High resolution light curves with a time resolution of 0.14 ms are generated. The Windowed Timing (WT) mode is obtained by binning and compressing 10 rows into a single row, and then reading out only the central 200 columns of the CCD. Therefore, it covers the central 8 arcminutes of the field of view and provides one dimensional imaging and full spectral capability with a time resolution of 1.8 ms. This mode is used for fluxes in the range 1–600 mCrab. The Photon Counting mode (PC) allows full spatial and spectral resolution for source fluxes below 1 mCrab with a timing resolution of 2.5 seconds.

X-ray events are classified according to the number and distribution of pixels in which they are detected, and are assigned ‘grades’ accordingly (XRT uses a library of grades which is derived from the XMM-Newton grading scheme). Default values of grades are 0–5 for PuPD and LrPD, 0–2 for WT and 0–12 for PC mode.

The on-ground calibration of the XRT effective area was carried out in 2002 Sep 23–Oct 4 at the Panter laboratory of the Max-Planck-Institut für extraterrestrische Physik where the integrated system was tested [**?**]. Here we describe the performance of the present Ancillary Response Files (ARF) generation that were improved, based on the spectroscopic study of several astronomical sources observed by XRT during the in-flight calibration phase, which ended on 2005 Apr 5, and later observations of some cosmic sources performed contemporaneously with XMM and RXTE observatories.

THE IN-FLIGHT CALIBRATION

The XRT effective area is the product of three components: i) the effective area of the mirror, ii) the quantum efficiency (QE) of the CCD and iii) the filter transmission.

In the specific case of XRT, the QE is included in the redistribution matrix (RMF) while the ARFs include the mirror effective area and filter transmission, as well as the vignetting correction and the Point Spread Function (PSF) correction, as a function of the source location and of the size of the extraction region.

We generated ARFs for LrPD, WT and PC XRT modes, and for different grade selections for each mode[1], as an improvement upon the on-ground ones. Based on our knowledge of well-known spectral distribution of some stable astrophysical sources, the on-ground ARFs were modified so that the resulting XRT spectrum becomes consistent with the observed ones through detailed modeling of the residuals. XRT effective area was calibrated using the Crab nebula (for LrPD and WT modes) and the SNR B0540-69 (PC mode). Here we report the performance for the default grade selections.

For the LrPD mode the the on-ground ARF was modified to reproduce spectral energy distribution with best fit parameters consistent with those reported in the literature and based on data collected by BeppoSAX (Massaro et al 2001) and RXTE (Pravdo et al 1997). Fig. 1 (top panel) shows the residuals obtained by fitting the Crab nebula spectrum with an absorbed power law. The reduced $\chi^2_{\rm red}$ is 1.5 (919 degrees of freedom, dof). The residual systematic uncertainty is lower than 5% level in the 0.6-10 keV energy range with a residual feature at the level of 5% at 5 keV. The flux measuments between XRT and BeppoSAX MECS produce a discrepancy of 2%.

The Crab rate produces, in WT mode, a moderate pile-up that we reduced extracting the off-pulse spectrum (mainly due to the nebula) with a phase-resolved selection. We modified the on-ground WT ancillary files to reproduce the off-pulse spectral model obtained by BeppoSAX-MECS (G. Cusumano, private comunication). Fig. 1 (middle panel) shows the residuals obtained by fitting the phase-resolved Crab nebula spectrum with an absorbed power law. The fit yields $\chi^2_{\rm red} = 1.4$ (943 dof). We estimate a residual systematic uncertainty lower than of 5% in the 0.3-10 keV energy range with a residual feature at the level of 10% around 0.7 KeV.

PC mode ARFs were calibrated with the SNR B0540-69 that, thanks its low count rate ($\sim$ 0.7 c/s) and moderate angular extension ($\sim$ 10-15 arcseconds), produce a negligeable pile-up. Fig. 1 (bottom panel) shows the residuals obtained by fitting the SNR spectrum with an absorbed power-law model + a non-equilibrium ionizzation model (NEI). The reduced $\chi^2_{\rm red}$ is 1.4 (943 degrees of freedom, dof). The statistical uncertainty is lower than 10% level in the 0.7-10 keV energy range, of the same order of the available statistics. Systematics residual are still present below 0.7 keV.

CONCLUSION

The in-flight calibration has allowed to improve the effective area files for all observing modes and grade selections to a level that satisfies the mission requirements. Further improvement of the ARFs, especially at the low energy end of the spectrum, is coming

[1] The adopted calibration method implies that in the CALDB ARF fi les we include the residual correction of the CCD quantum effi ciency. This explains why the nominal ARF fi les are different for different grade selections.

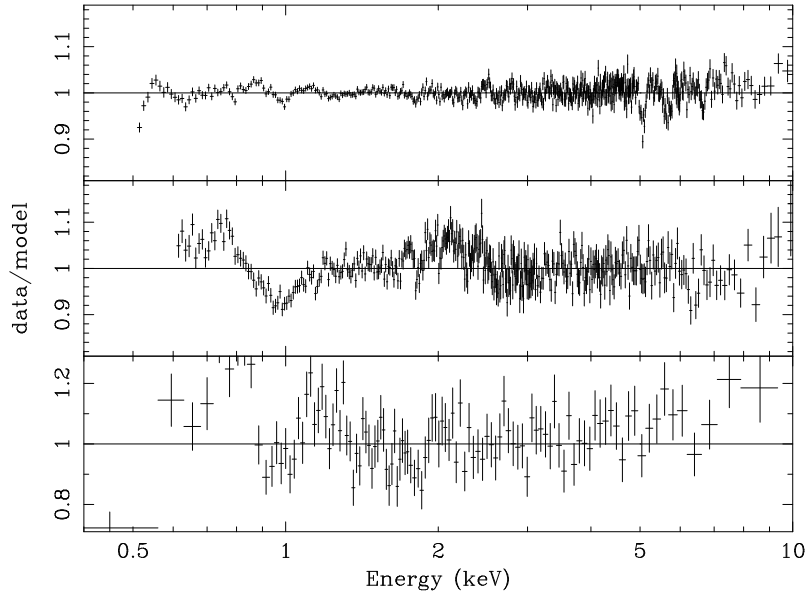

FIGURE 1. Top panel (LrPD mode): residuals obtained by fitting the Crab nebula spectrum with an absorbed power law. Middle panel (WT mode): residuals obtained by fitting the phase-resolved off-pulse Crab nebula spectrum with an absorbed power law. Bottom panel (PC mode): residuals obtained by fitting the SNR 0540-69 spectrum with an absorbed power-law model + a non-equilibrium ionizzation model (NEI).

with the use of more calibration sources and by using XRT and XMM-Newton contemporaneous source observations.

ACKNOWLEDGMENTS

The authors acknowledge support from ASI, NASA and PPARC.

REFERENCES

1. N., Gehrels, G., Chincarini, P., Giommi, et al., *Astrophys. J.* **611**, 1005-1020 (2004)
2. S., Barthelmy, L.M., Barbier, J.R., Cummings, et al., *Space Sci. Rev.*, **120**(2005)
3. D.N., Burrows, J.E., Hill, A., Nousek, et al., *Space Sci. Rev.*, **120**(2005)
4. P.W. Roming, et al., *Space Sci. Rev.*, **120**(2005)
5. O., Citterio, S., Campana, P., Conconi, et al., *Proc. SPIE*, **2805**, 54-65 (1996)
6. D.N., Burrows, J.E., Hill, A., Nousek, et al., *Proc. SPIE*, **4851**, 1320-1325 (1996)
7. G., Tagliaferri, M., A.Moretti, S. Campana, et al., *Proc. SPIE* **5165**, 241-250 (2004)
8. E., Massaro, M., Litterio, G., Cusumano al., *Integral Workshop 4-8 September 2000*, 229-233 (2001)
9. S.H., Pravdo, G., L., Angelini and A.K. Harding, *Astrophys. J.*, **491**, 808-815 (1997)